IEEE Access
Multidisciplinary ⋮ Rapid Review ⋮ Open Access Journal

Received 26 April 2023, accepted 23 May 2023, date of publication 29 May 2023, date of current version 7 June 2023.

Digital Object Identifier 10.1109/ACCESS.2023.3280850

RESEARCH ARTICLE

Hybrid Optical Wireless Communication for Versatile IoT Applications: Data Rate Improvement and Analysis

SHIVANI RAJENDRA TELI[1], CARLOS GUERRA-YANEZ[1], VICENTE MATUS ICAZA[2], RAFAEL PEREZ-JIMENEZ[2], ZABIH GHASSEMLOOY[3], (Senior Member, IEEE), AND STANISLAV ZVANOVEC[1], (Senior Member, IEEE)

[1]Department of Electromagnetic Field, Faculty of Electrical Engineering, Czech Technical University in Prague, 16627 Prague, Czech Republic
[2]Institute for Technological Development and Innovation in Communications, Universidad de Las Palmas de Gran Canaria, 35001 Las Palmas, Spain
[3]Optical Communications Research Group, Faculty of Engineering and Environment, Northumbria University, NE1 8ST Newcastle upon Tyne, U.K.

Corresponding author: Shivani Rajendra Teli (telishiv@fel.cvut.cz)

This work was supported in part by the Czech Technical University (CTU) in Prague under the CTU Global Postdoctoral Fellowship Program, in part by the European Cooperation in Science and Technology (COST) Action CA19111 (Newfocus), and in part by CTU under Project SGS23/168/OHK3/3T/13.

ABSTRACT This paper outlines the concept of a multilevel bipolar on-off keying hybrid optical wireless communication (OWC) system using a single light-emitting diode (LED) as a transmitter as well as photodiode and camera-based receivers for versatile indoor Internet of Things applications. The proposed system offers simultaneous high- and low-speed transmission capabilities using visible light communication (VLC) and optical camera communication (OCC) links, respectively. By means of experimental implementation, we show that the hybrid OWC system employing a chip LED modulated with a multilevel signal improves the data rate R_b as well as the bit error rate and reception success rate of VLC and OCC links, respectively, by doubling the bandwidth. We show that the proposed scheme can provide an independent link performance, irrespective of significant differences between the operating R_b of VLC and OCC over a range of transmission spans L. We demonstrate that the throughput of the VLC link is improved by up to ∼100 Mb/s, which corresponds to twice the LED bandwidth, using direct modulation, different amplitude levels, and optimizing the received optical power of the hybrid OWC link. Error-free data transmission for the OCC link is achieved for all values of R_b, amplitude overlap of 0 and 0.3, and a range of L.

INDEX TERMS Optical wireless communications (OWC), visible light communications (VLC), optical camera communications (OCC), Internet of Things (IoT), light emitting diodes (LEDs), photodiode (PD).

I. INTRODUCTION

Hybrid wireless systems, such as radio frequency (RF)-optical and all-optical, are seen as excellent solutions for Internet of Things (IoT) applications in the emerging sixth-generation communication network and beyond [1], [2], [3]. In the optical wireless communication (OWC) domain, we have the possibility of utilizing a combination of visible light communication (VLC), optical camera communication (OCC), and free space optical (FSO) technologies in both indoor and outdoor environments. In recent years, we have seen the introduction of all-optical hybrid wireless technologies in IoT, including:

(i) FSO-VLC [4], [5]: This hybrid system, utilizing both infrared and visible bands, has been gaining popularity for use in the last-meter (i.e., mostly indoor) and last-mile (i.e., outdoor) access networks because of higher data rates R_b, enhanced security, and performance. In [4], an experimental multiband carrier-less amplitude and phase hybrid optical system was proposed, where FSO and VLC were used for last mile and last meter sections. A hybrid optical wireless network

The associate editor coordinating the review of this manuscript and approving it for publication was Barbara Masini.

with VLC-FSO-VLC configuration within a heterogeneous interconnection was experimentally investigated for possible use in space-air-ground-ocean-integrated communication architecture [5].

(ii) VLC-OCC [6], [7], [8], [9], [10], [11]: In many indoor IoT applications, such as identification and promotion information, control signals, and indoor localization, where R_b is very low, a hybrid VLC-OCC system would be an excellent option to meet the necessary requirements [6], [7], [8]. This option effectively utilizes the light emitting diode (LED)-based lighting infrastructure and cameras in smart devices and in CCTV as the optical transmitter (Tx) and the receiver (Rx), respectively [9]. Note OCC-based systems are attractive for IoT applications where a higher signal-to-interference-plus-noise ratio (SINR) and lower bit error rates (BERs) are more critical than higher R_b. On the other hand, for high-speed downloading (i.e., internet surfing and online streaming), VLC utilizing a fast optical photodetector (PD) would be the preferred option [8]. In [10] and [11], a theoretical model of a hybrid VLC-OCC system based on the selection of access points using fuzzy logic for network selection, i.e., either OCC or VLC, was proposed. A switching mechanism was used to select the OCC or VLC link (but not both), based on the network selection factor obtained using fuzzy logic and extended further using fuzzy logic and round-robin scheduling for assigning an appropriate network to the users.

Note that, in the practical implementation of hybrid VLC-OCC schemes, there are a few issues that must be addressed, including (*i*) a huge bandwidth B difference between cameras and PD-based Rxs; [6], [7]; (*ii*) higher attenuation at a lower frequency range due to the use of a high-pass filter-based LED driver [8]; (*iii*) high light intensity, which is desirable in VLC but not required in OCC [6]; (*iv*) the impact of ambient light-induced interference; (*v*) complexity and implementation costs; and (*vi*) integration with existing/future networks.

In this work, we aim to address some of the above-mentioned challenges in [6], [7], [8], [9], [10], and [11] by investigating a bipolar on-off keying (OOK) single-input multiple-output (SIMO) hybrid OWC scheme, which utilizes a single LED-based Tx, as well as PD- and camera-based Rxs for high- and low-speed VLC and OCC links, respectively. An experimental testbed for a static SIMO VLC-OCC downlink was developed in [8], where it was shown that the use of a bias-T with a high-pass filter feature resulted in increased attenuation in both VLC and OCC links, *i.e.*, resulting in lower SNR and, subsequently, higher BER and lower reception success rate R_{rs}, respectively. Therefore, in this paper, we propose a hybrid OWC scheme with direct modulation of the chip LED using drive voltage V_d levels (*i.e.*, peak-to-peak voltage V_{pp} and offset voltage V_{os}) to mitigate the attenuation, thereby increasing B. A lens will also be used to improve the power levels at both the Tx and the Rx. The novelty of this work lies in the results obtained, including (*i*) double R_b to 100 Mb/s for a high-speed VLC link compared with [8], which is, to the best of our knowledge, reported for the first time in hybrid OWC links; (*ii*) improved R_{rs} by 100 % (*i.e.*, error-free transmission) for a low-speed OCC link; and (*iii*) a demonstration that the performance of links are independent of each other, as opposed to the results in [8], which illustrates the trade-off between the performance of VLC and OCC links. Performance results are presented in terms of the BER and R_{rs} for VLC and OCC links, respectively, for a range of transmission spans L and different camera orientations in terms of the camera offset C_{off}.

The remaining sections are organized as follows: Section II provides an overview of the proposed hybrid OWC system; Section III presents experiment results and discussion; and Section IV concludes the article with an outlook towards future work.

II. HYBRID OWC: SYSTEM OVERVIEW

The schematic block diagram of the hybrid OWC scheme for simultaneous data transmission of high- and low-speed signals $x_{\text{hs}}(t)$ and $x_{\text{ls}}(t)$, respectively, is shown in the Tx block of Fig. 1. The hybrid bipolar OOK signal is generated by superimposing high- and low-speed signals, which is given as:

$$x_{\text{bp}}(t) = x_{\text{hs}}(t) + x_{\text{ls}}(t), \tag{1}$$

$x_{\text{hs}}(t)$ and $x_{\text{ls}}(t)$ can be defined as:

$$x_{\text{hs}}(t) = \text{Signal}\left(f_{s\text{-High}}\right)_{T_{b\text{-High}}}, \tag{2}$$

$$x_{\text{ls}}(t) = \text{Signal}\left(f_{s\text{-Low}}\right)_{T_{b\text{-Low}}}, \tag{3}$$

where $f_{s\text{-High}}$ and $T_{b\text{-High}}$ are the modulation frequency and bit duration of $x_{\text{hs}}(t)$, respectively, $f_{s\text{-Low}}$ and $T_{b\text{-Low}}$ are the modulation frequency and bit duration of $x_{\text{ls}}(t)$, respectively. Note, $x_{\text{bp}}(t)$ resembles the bipolar codes widely used in traditional wireless code division multiple access (CDMA) systems [12] with the merits of good correlation functions, thus making it easier to effectively distinguish users in multi-user scenarios and mitigate multipath interference [12]. Here, we have considered (*i*) a fixed 10-bit long data packet format of [0011011001] for $x_{\text{ls}}(t)$, which can be replaced with CDMA codes to support a multi-user environment; and (*ii*) data rates of $10 < R_{b\text{-High}} < 100$ Mb/s with a step of size 10 Mb/s for the high-speed VLC link as well as $R_{b\text{-Low}}$ of 1, 2, and 5 kb/s for the low-speed OCC link.

$x_{\text{bp}}(t)$ is generated in MATLAB and uploaded to the arbitrary waveform generator (AWG Teledyne test tools T3AWG3252 with a sampling frequency of 1 GS/s), the output of which is used for intensity modulation of the chip LED, see the Tx block in Fig. 1. A commercially available Tx ultrabright super-thin red chip LED-based is used with a typical wavelength λ_p of 630 nm (Vishay VLMS1500-GS08), which is biased at bias current I_b of 90 mA and

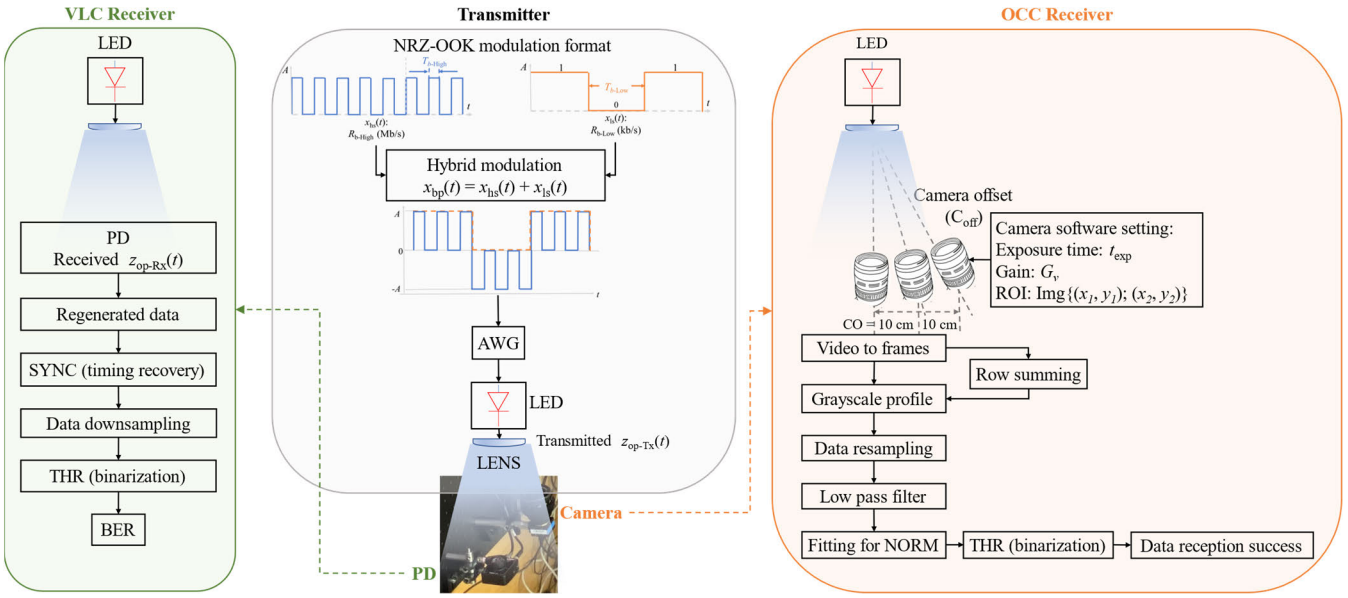

FIGURE 1. A hybrid OWC transmission system for IoT. Note that, 'SYNC', 'THR', 'BER', 'ROI' and 'NORM' blocks refer to synchronization, thresholding, bit error rate, region-of-interest, and normalization, respectively.

drive voltage V_d levels corresponding to a transmit output power P_t of ∼3.3 mW [13]. The modulated optical signal $z_{\text{op-Tx}}(t)$ is transmitted over a free-space channel of length L using a collimated lens with a length $f_{c\text{-Tx}}$ of 11 mm. Note, both direct intensity modulation of the LED and using collimating lenses at the Tx and the Rx lead to reduced signal attenuation due to the high-pass filtering of the bias-T [8]. At the Rx, a collimating lens with a length $f_{c\text{-Tx}}$ of 16 mm was used to focus the incoming light onto a PD.

At the Rx side, both camera- and PD-based Rxs are used to capture the received signal $z_{\text{op-Rx}}(t)$ containing both the attenuated versions of $x_{\text{ls}}(t)$ and $x_{\text{hs}}(t)$. Accordingly, we have proposed a solution based on A overlap A_{OL}, see Fig. 2, to increase signal levels (*i.e.*, A-depth) and therefore improve BER performance of high-speed signal $x_{\text{hs}}(t)$ as well as maintain the high quality of low-speed signal $x_{\text{ls}}(t)$. At $A = 0$, A_{OL} is the increase in the A level on both the $+A$ and -A levels. The variations in the signal levels of $x_{\text{hs}}(t)$ and $x_{\text{ls}}(t)$ with A_{OL} can be defined as:

$$A_{\text{hs}} = A + \frac{A_{\text{OL}}}{2}, \quad A_{\text{ls}} = A - \frac{A_{\text{OL}}}{2}, \tag{4}$$

where, $A_{\text{OL}}/2$ is the result of increasing the level of A_{OL} for both positive and negative signals, see Figs. 2(a) and (b), which illustrate the examples of measured $z_{\text{op-Rx}}(t)$ for an L of 1 m, P_r of 0.2 dB, and A_{OL} of 0 (*i.e.*, no overlapping between the voltage levels) and 0.3. We have shown that A_{OL} increases the total amplitude depth A of the VLC signal at the cost of deteriorating $x_{\text{ls}}(t)$ performance. This is explained in Section III.

For the data processing of the VLC link with the PD, we need to determine the time delay between the transmitted and received signals to ensure synchronization. The process is followed by the down-sampling of the received signal and thresholding for data decoding. The received data bit

TABLE 1. Key measurement parameters.

Parameter	Description	Value
Red LED		**Vishay VLMS1500-GS08**
I_b	Bias current	90 mA
P_t	Transmit optical power	3.3 mW
l-max	Luminous	180 mcd
$B_{\text{LED-3dB}}$	LED bandwidth	< 50 MHz
PD Rx		**Thorlabs PDA10A2**
wavelength		200 – 1100 nm
B_{PD}	PD bandwidth	1 GHz
active area		0.8 mm^2
Optical lens		**Thorlabs ACL25416U**
$f_{c\text{-Tx}}$,$f_{c\text{-Rx}}$	Focal lengths at the Tx and the Rx	11 and 16 mm
Camera Rx		**IC capture 2.4 imaging source2**
resolution		648×484 pixels
f_R	Camera frame rate	25 fps
t_{exp}	Exposure time	200 µs
G_v	Camera gain	16 dB
$R_{b\text{-High}}$	VLC data rate	10:10:100 Mb/s
data length		6×10^6
$R_{b\text{-Low}}$	**OCC data rate**	**1, 2 and 5 kb/s**
data length		10 bits superimposed over $R_{b\text{-High}}$
L	Transmission distance	1–4 m
P_r	Optical power at the Rx	0.2 dBm **(L = 1 m), -3.8** dBm **(2 m),** -7.5 dBm (3 m) and -9.9 dBm (4 m)
C_{off}	Camera offset	0, 10 and 20 cm

stream $x_{\text{hs-Rx}}(t)$ is compared with the $x_{\text{hs}}(t)$ to determine the BER. We optimized the beam collimation at the Tx by monitoring received optical power P_r at the PD for a range of L with a step of size 1 m. The measured P_r were about 0.21 and −9.9 dB at transmission distances of 1 and 4 m, respectively. Table 1 shows the key system parameters adopted in this work. Here, we have used a red chip LED as the Tx, with the option of adding green and blue LEDs to produce white light for simultaneous illumination and data communication. Unlike the optical-hybrid schemes proposed in [6], [7], [10], and [11], the advantage of the simultaneous transmission of $x_{\text{hs}}(t)$ and $x_{\text{ls}}(t)$ is to improve the data throughput by increasing B and link quality in terms of BER.

Figure 3 shows the frequency response of bias-T and the captured $z_{\text{op-Tx}}(t)$ with and without bias-T. The insets in Fig. 3 illustrate highly attenuated received $x_{\text{hs}}(t)$ signals for an $R_{b\text{-Low}}$ of 1 kb/s, which lead to reduced A and, hence, increased BER. Note that, (*i*) at higher frequencies, the effect of bias-T acting as a high pass filter is negligible; and (*ii*) attenuation due to bias-T is completely mitigated with the intensity modulation of the LED and by the characterization of the lens.

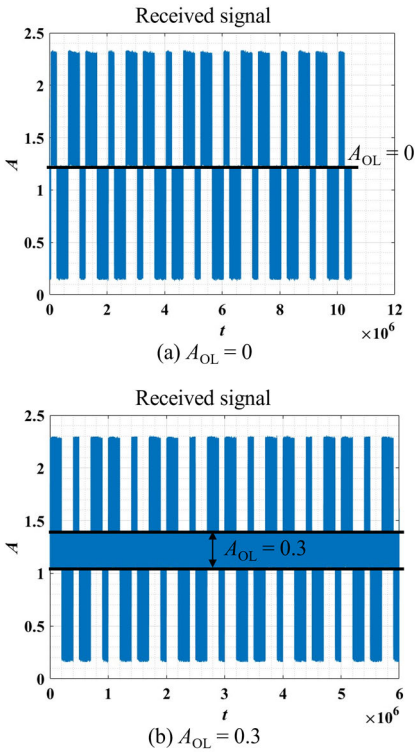

FIGURE 2. Received $z_{\text{op-Rx}}(t)$ on oscilloscope from PD at $L = 1$ m.

In the OCC link, a rolling-shutter (RS)-based camera was used to capture $x_{\text{ls}}(t)$ to ensure flicker-free transmission with improved data throughput regardless of f_R, which is 25 fps [15]. The camera was controlled using IC capture

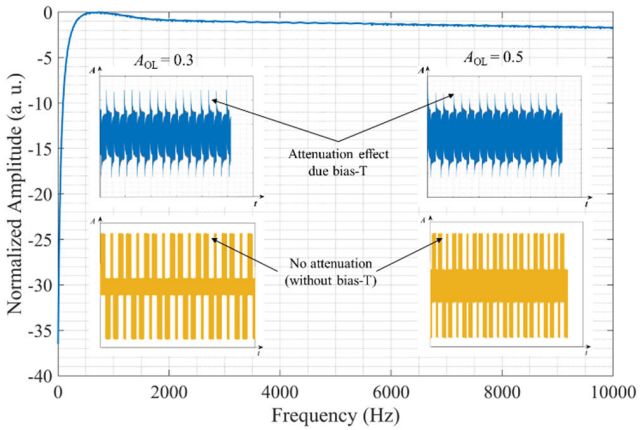

FIGURE 3. The frequency response of bias-T and measured $z_{\text{op-Rx}}(t)$ at $R_{b\text{-Low}} = 1$ kb/s. Note, the blue waveform represents an attenuated signal due to bias-T [8] and the yellow waveform represents the received waveform without bias-T (no attenuation).

2.4 software for further offline data processing in MATLAB based on widely used image processing techniques, see the OCC Rx block in Fig. 1. Here, we utilized the software-based camera control to set the capturing parameters of the region-of-interest (ROI), as well as gain G_v, exposure time t_{exp}, and resolution of 16 dB, 200 μs, and 648 × 484 pixels, respectively, while recording the data. Note, ROI was set considering the most uniform intensity levels in the capture frames to avoid reflections from the lens positioned in front of an LED. Figure 4 depicts six examples of the grayscale intensity profiles of captured image frames of video streams with a duration of 2 s for a range of A_{OL}, C_{off}, and $R_{b\text{-Low}}$. Note, the intensity levels of received $x_{\text{ls}}(t)$ are marginally affected at higher values of A_{OL}, *i.e.*, with an increase in A_{OL}, there is a marginal decrease in the overall grayscale intensity profiles of the captured low-speed signal, see Fig. 4(a). In general, this is due to the overall reduction in $+A$ as a result of the increase in A_{OL}(*i.e.*, corresponds to $A - \frac{A_{\text{OL}}}{2}$), see (4). Figure 4(b) illustrates the examples of

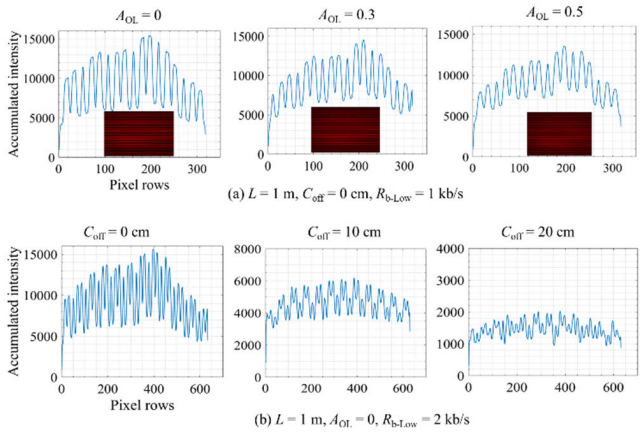

FIGURE 4. Received OCC signals in the image frames.

captured images for C_{off} of 0, 10, and 20 cm and $R_{b\text{-Low}}$ of 2 kb/s. The reduction in intensity levels can be noticed as the camera is no longer in the direct line-of-sight (LOS) path of the LED, *i.e.*, $C_{\text{off}} > 0$, see the OCC Rx block in Fig. 1.

The captured video stream is divided into image frames for further processing to decode the received data stream. The captured frames are then converted from RGB to grayscale to eliminate the hue and saturation information while retaining the luminance of the image plane and are used to retrieve the intensity profiles. The intensity profiles are normalized for thresholding and binarization of the data frames and converting them to a vector transformation for decoding the data streams. For this reason, we have adopted curve fitting techniques as described in [15], which is explained in Section III: Experiment results and discussions, with examples of data processing on captured image frames, are also outlined in Section III. Finally, the received data bit vector is compared with the transmitted data bit stream to evaluate the R_{rs} of the received bits by determining the ratio of the correctly decoded against the total number of transmitted bits.

III. EXPERIMENT RESULTS AND DISCUSSIONS

We developed an experimental testbed, see Fig. 5, for the proposed system and evaluated its performance in terms of BER and R_{rs} by considering the effects of $R_{b\text{-Low}}$ and $R_{b\text{-High}}$ on OCC and VLC links, respectively, using the parameters listed in Table 1. For $x_{\text{hs}}(t)$ with the reference signal (i.e., unipolar OOK signal to measure only $x_{\text{hs}}(t)$), we have adopted the well-known strategy of zero-padded-based guard intervals as the header [13], [14] to obtain the real-valued signal. Tests were carried out for a link span range of $1 < L < 4$ m with a step of size 1 m and for $10 < R_{b\text{-High}} < 100$ Mb/s with a step of size 10 Mb/s for $x_{\text{hs}}(t)$. Figure 6 depicts examples of captured eye diagrams of received error-free independent (unipolar OOK) high-speed $x_{\text{hs}}(t)$. The figure shows a two-level OOK signal with a wide eye-opening representing an error-free transmission. Note that the eye-opening reduces with increasing $R_{b\text{-High}} > 50$ Mb/s, which corresponds to the LEDs' frequency response (i.e., $B_{\text{LED-3dB}} < 50$ MHz).

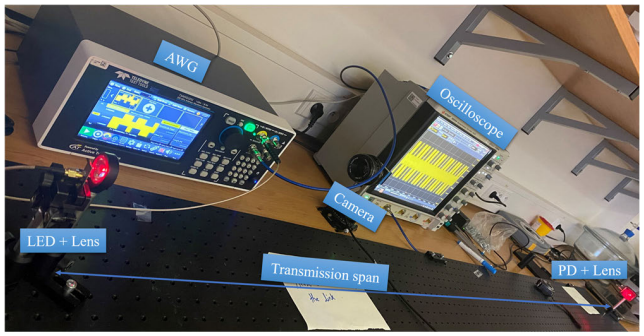

FIGURE 5. Hybrid OWC scheme: Experiment setup. Note, camera is set to $C_{\text{off}} = 20$ cm at $L = 1$ m and PD is set at $L = 3$ m.

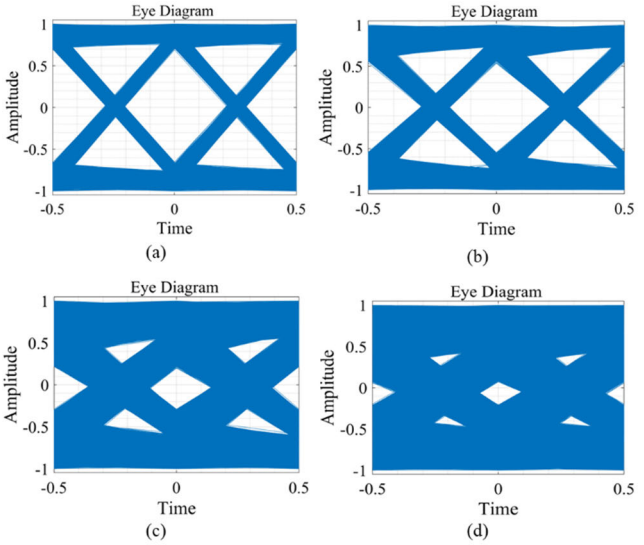

FIGURE 6. Eye diagrams of received error-free independent (unipolar OOK) high-speed VLC link at $R_{b\text{-High}}$ for: (a) 20 Mb/s, (b) 40 Mb/s, (c) 80 Mb/s, and (d) 100 Mb/s.

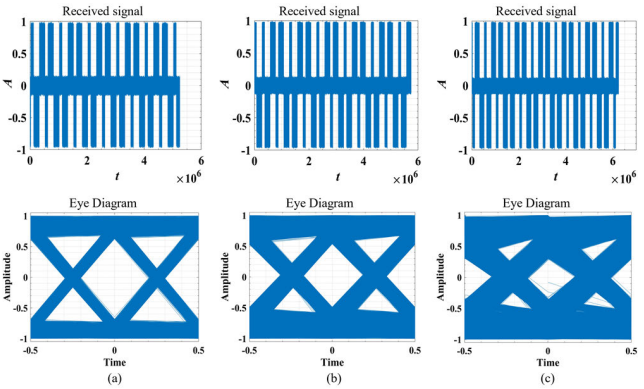

FIGURE 7. Received signals (up) and eye diagrams (bottom) of $x_{\text{hs}}(t)$ at $A_{\text{OL}} = 0.3$, $R_{b\text{-Low}} = 2$ kb/s, L of 2 m and: (a) $R_{b\text{-High}} = 10$ Mb/s; (b) $R_{b\text{-High}} = 30$ Mb/s, and (c) $R_{b\text{-High}} = 50$ Mb/s.

To analyze the performance of the VLC link with respect to the OCC link in the proposed hybrid OWC scheme with $x_{\text{bp}}(t)$, see Fig. 1, we have considered three main parameters of (*i*) $R_{b\text{-High}}$ in the range of 10 – 100 Mb/s with a step of size 10 Mb/s; (*ii*) $R_{b\text{-Low}}$ of 1, 2, and 5 kb/s; and (*iii*) A_{OL} of 0, 0.3, and 0.5. In Fig. 7, eye diagrams illustrate the error-free data transmission achieved up to $R_{b\text{-High}}$ of 50 Mb/s at $A_{\text{OL}} = 0.3$, $R_{b\text{-Low}} = 2$ kb/s and L of 2 m for $x_{\text{hs}}(t)$ using a hybrid bipolar modulation format. For $R_{b\text{-High}} > 50$ Mb/s (60-100 Mb/s), the performance is not error-free since $B_{\text{LED-3dB}}$ is < 50 MHz; therefore, we have evaluated the BER performance of the VLC link as a function of $R_{b\text{-High}}$ for a range of $R_{b\text{-Low}}$, L, and A_{OL} as shown in Fig. 8. Also shown are the forward error correction (FEC) and BER_{min} limits. Note BER_{min} refers to the resolution limit adopted in the error detection estimation and is set to 1.667×10^{-6}(1/no. of bits transmitted), which is determined by the length of

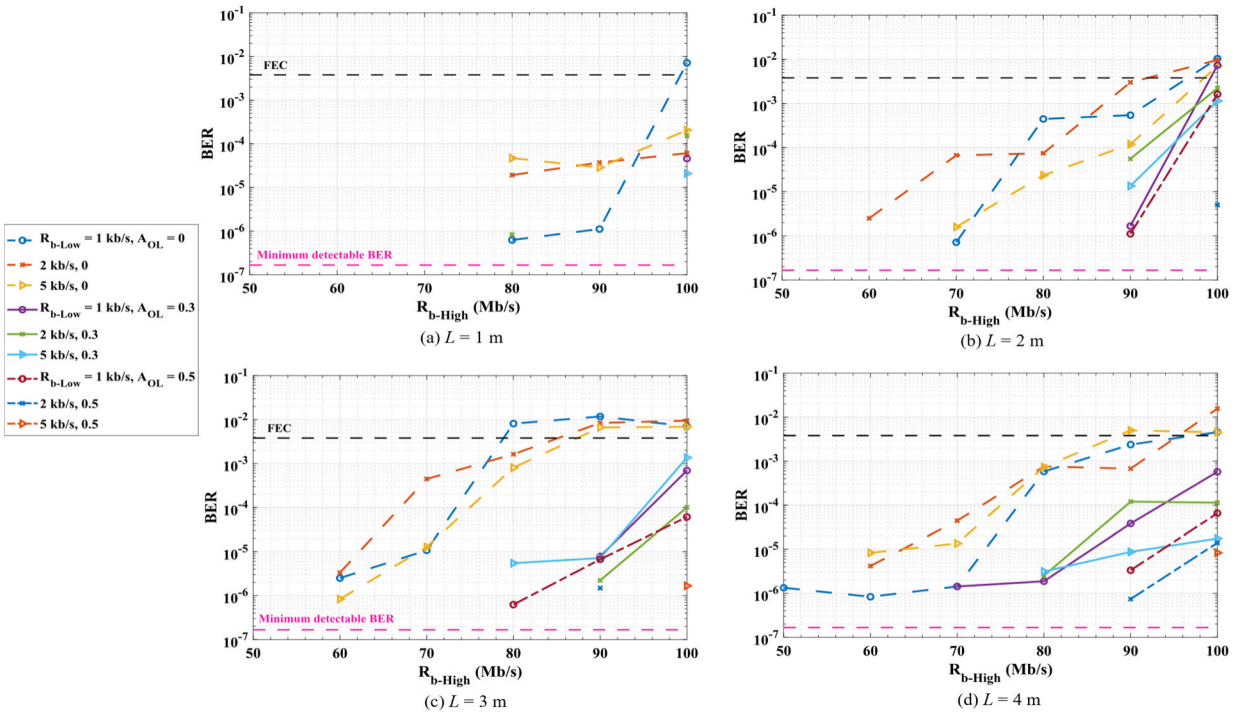

FIGURE 8. VLC link performance analysis in terms of BER with respect to L, $R_{b\text{-High}}$, $R_{b\text{-Low}}$ and A_{OL}.

TABLE 2. Performance analysis of the OCC link: Reception success in %.

L (m)	A_{OL}	$R_{b\text{-Low}}$ (kb/s) \ C_{off} (cm)	0	10	20
3	0	1	100	100	99.6
		2	99.4	99.4	99.3
		5	90.3	88.0	86.4
	0.3	1	100	100	99.0
		2	99.2	98.9	98.6
		5	90.0	86.1	85.0
	0.5	1	100	-	-
		2	99.1	-	-
4	0	1	100	100	98.6
		2	99.3	98.6	97.7
		5	87.8	86.0	85.0
	0.3	1	100	100	98.5
		2	99.1	98.5	97.3
		5	85.6	84.0	83.1
	0.5	1	99.6	-	-
		2	98.9	-	-

the generated bit stream. For L of 1 m, and all values of $R_{b\text{-Low}}$, we observe BER plots are well below the FEC limit of 3.8×10^{-3} for $10 < R_{b\text{-High}} < 90$ Mb/s, see Fig. 8(a). It can be seen that (*i*) using direct modulation, different V_d levels, and optimizing the received optical power, error-free transmission can be achieved up to $R_{b\text{-High}}$ of 50 Mb/s for all values of L, corresponding to B_{LED} of 50 MHz; (*ii*) the BER for $x_{\text{hs}}(t)$ is between the FEC and minimum detectable BER limits for L of 2 up to 4 m, $R_{b\text{-Low}}$ of 2 kb/s, A_{OL} of 0.3 and 0.5, and $R_{b\text{-High}}$ of 40 and 100 Mb/s, see Figs. 8(b), (c) and (d); (*iii*) errors increase with an increase in $R_{b\text{-High}}$, which is expected due to limited B_{LED} (*i.e.*, lower than 50 MHz), and (*iv*) errors decrease with increasing $R_{b\text{-Low}}$ and A_{OL}, which corresponds to an increase in amplitude levels of $x_{\text{hs}}(t)$ and the quality of the link, see (4).

As with the VLC link, we first measured $x_{\text{ls}}(t)$ with the reference signal at $R_{b\text{-Low}}$ of 1, 2 and 5 kb/s with respect to all values of $R_{b\text{-High}}$ and A_{OL}. In our measurement campaign, we recorded a 2 s-long video (at f_R of 25 fps) of the intensity modulated light, where six repeated 10-bit long [0011011001] data packets per every image frame were captured at $R_{b\text{-Low}}$ of 1, 2 and 5 kb/s, respectively. Considering the lower number of bits being transmitted, OCC performance was analyzed in terms of R_{rs}, which is defined by the ratio of correctly decoded bits to the total number of transmitted bits. Note, for the reference OCC link R_{rs} of 100 % (i.e., error-free transmission) and 95 % were achieved at $R_{b\text{-Low}}$ of 1–2 and 5 kb/s, respectively.

In contrast to the results given in [8], which depicted the performance trade-off between VLC and OCC links, in the proposed hybrid OWC link, we show that link performances are independent of each other. Therefore, for OCC, we set $R_{b\text{-High}}$ to 50 Mb/s (due to $B_{\text{LED-3dB}}$ of < 50 MHz and error-free performance of $x_{\text{hs}}(t)$ up to 50 Mb/s for all values of $R_{b\text{-Low}}$, A_{OL}, and L) and measured the link performance for $R_{b\text{-Low}}$ of 1, 2 and 5 kb/s and all values of A_{OL} and

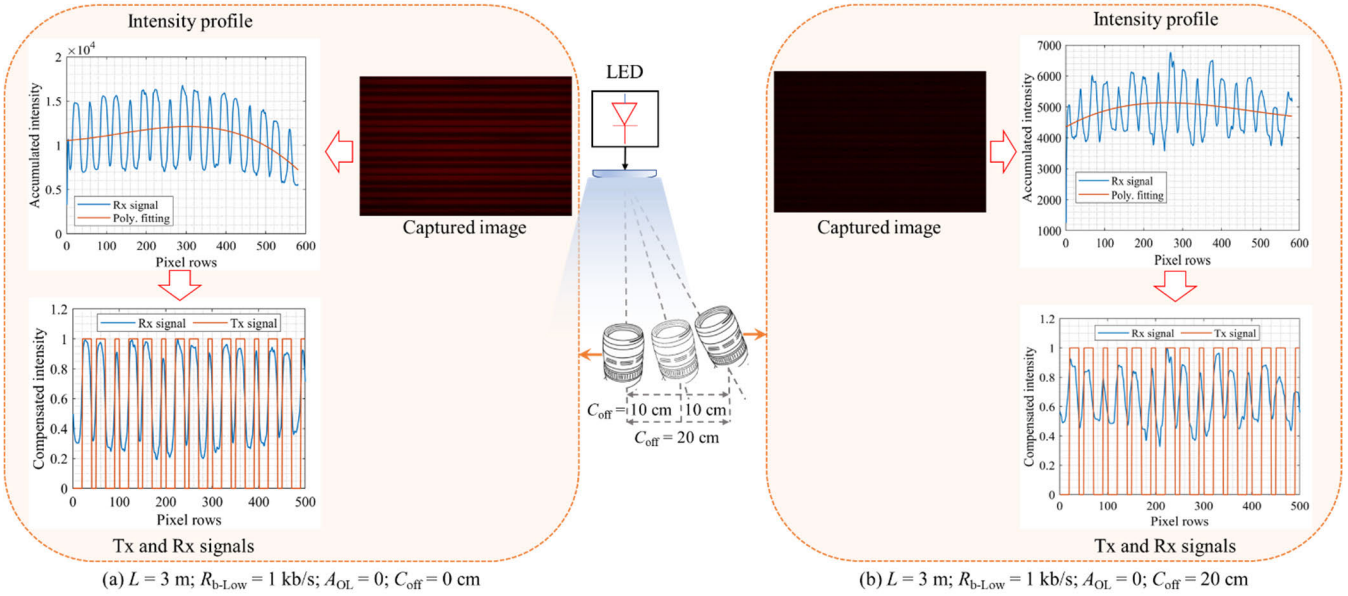

(a) L = 3 m; $R_{b\text{-Low}}$ = 1 kb/s; A_{OL} = 0; C_{off} = 0 cm

(b) L = 3 m; $R_{b\text{-Low}}$ = 1 kb/s; A_{OL} = 0; C_{off} = 20 cm

FIGURE 9. OCC data processing using grayscale intensity profiles.

C_{off}. Figure 9 illustrates examples of signal processing for the OCC link based on the grayscale intensity profiles and fitting techniques for $R_{b\text{-Low}}$ of 1 kb/s, L of 3 m, and C_{off} of 0 and 20 cm, see Fig. 9(a) and (b), respectively. Note, (*i*) here we have used the 4th-degree polynomial fitting technique (due to the curved nature of intensity profiles because of the circular LED shape) to normalize the original grayscale data pattern as in [15]; (*ii*) the intensity levels of received $x_{ls}(t)$ are marginally affected at higher values of A_{OL}, which correspond to reduced A, see Fig. 4(a); (*iii*) the intensity profiles are largely reduced with increasing C_{off}, as shown in Figs. 4(b) and 9(b); and (*iv*) the transmitted and received signals show a good match. 100 % (error-free transmission) and ∼92 % of R_{rs} are achieved at $R_{b\text{-Low}}$ of 1–2 and 5 kb/s, respectively, A_{OL} of 0 and 0.3, C_{off} of 0, 10, and 20 cm, and L of up to 2 m. This is due to the fact that the LED acts as a low pass filter, thus providing a good signal reception even at lower R_{b-Low} [13]. For an A_{OL} of 0.5 and L of up to 2 m, the 100 % R_{rs} is achieved at $R_{b\text{-Low}}$ of 1 kb/s, while for $R_{b\text{-Low}}$ of 2 kb/s R_{rs} is reduced to ∼96 %. Table 2 shows the values of R_{rs} for the OCC link for a range of $R_{b\text{-Low}}$, A_{OL}, C_{off}, and L. It can be seen that R_{rs} of 100 % is achieved at $R_{b\text{-Low}}$ of 1 kb/s for all values of A_{OL} and C_{off}. Note, R_{rs} (*i*) is further reduced to 97 and 83 % for $R_{b\text{-Low}}$ of 2 and 5 kb/s, respectively, and L of 4 m; and (*ii*) was not measured for $R_{b\text{-Low}}$ of 5 kb/s at A_{OL} of 0.5 and C_{off} of 10 and 20 cm due to the reduction in intensity levels of the captured image frames caused by moving the camera Rx apart in the LOS scenario, and reduced A when increasing A_{OL}.

To summarize the performance of the proposed hybrid OWC scheme with direct modulation, different V_d levels, and optimization of the received optical power, we have: (*i*) improved the VLC link's throughput by up to ∼100 Mb/s, which is equivalent to 2×$B_{LED\text{-}3dB}$; (*ii*) demonstrated that at A_{OL} of 0.3, the high-speed VLC link performance, in terms of BER, is well below the FEC limit for all values of L, $R_{b\text{-High}}$, and $R_{b\text{-Low}}$; (*iii*) shown that for of the low-speed OCC link with A_{OL} of 0.3, the average performance in terms of R_{rs} are 100, 97, and 85 % for $R_{b\text{-Low}}$ of 1, 2, and 5 kb/s, respectively for all values of L, $R_{b\text{-High}}$, and C_{off}; and (*iv*) demonstrated that the performances of the links are independent of each other unlike, and as opposed to, the results in [8] which illustrates the trade-off between the performance of the VLC and OCC links.

Finally, in Table 3, we compare the performance of the proposed hybrid OWC system with other schemes of VLC-OCC [6], [7], SIMO VLC [8], and hybrid OWC schemes with fuzzy logic [10], [11]. In [6], using a high power (15 W) LED lamp-based Tx and variable pulse position modulation (VPPM), L of 4 m and 5.8 m for VLC and OCC links, respectively, were reported. Based on intensity shift keying modulation formats, the L of 5 m using a 50 cm^2 rectangular LED panel with a 39 dBm power level and multilevel OOK was reported in [7]. However, no analysis to improve B was provided, so R_b, as well as the effect of multilevel LED transmission based on varying amplitude depths of $z_{op\text{-}Rx}(t)$, were reposted. The fuzzy logic-based networking schemes in [10] and [11] were designed to perform two separate switching of the links based on the network selection factor. Note that both technologies (*i*) were not expected to be used at the same time nor to employ a common Tx; and (*ii*) lacked details on simultaneous data transmission and processing algorithms considering modulation/demodulation formats, data reception and recovery, and BER performance. In [8], it was shown that the use of a bias-T with a high-pass filter feature resulted in increased attenuation in both links,

TABLE 3. Summary of existing hybrid schemes.

Schemes / Parameter	VLC-OCC [6]	VLC-OCC [7]	SIMO hybrid VLC [8]	Fuzzy logic-based networking in hybrid VLC-OCC [10, 11]	Proposed hybrid OWC scheme
Tx	15-W LED lamp	Rectangular LED panel 50cm^2 with 39 dBm power level	Thin red chip LED of the size 1.0 x 0.5 x 0.35 mm^3 ($B_{\text{LED-3dB}}$ < 50 MHz) with 3.3 mW transmit optical power	Simulation model: 10 W, 5 cm radius LED	Thin red chip LED of the size 1.0 x 0.5 x 0.35 mm^3 ($B_{\text{LED-3dB}}$ < 50 MHz) with 3.3 mW transmit optical power
Rx	VLC: PD (S6869) OCC: USB camera (f_R = 60 fps)	VLC: PD OCC: Google Pixel-2	VLC: Thorlabs PDA10A2 (1 GHz) OCC: USB camera (f_R = 25 fps)	Simulation model: VLC: 1 cm^2, 20 MHz PD; OCC: 30fps camera	VLC: Thorlabs PDA10A2 (1 GHz) OCC: USB camera (f_R = 25fps)
Modulation	Manchester coding and VPPM was used for OCC and VLC, respectively	Intensity shift keying and multilevel OOK	Bipolar multilevel OOK signal	Fuzzy logic-based networking for network switching techniques. Missing modulation and demodulation techniques	Bipolar multilevel OOK signal and direct modulation with driving voltage levels and lens characterization
L (m)	VLC: 4; OCC: 5.8	5	1	15 (simulation model)	$1 < L < 4$
$R_{b\text{-High}}$ (Mb/s)	0.1	2.75	Up to 35	Up to 1	Up to 100
$R_{b\text{-Low}}$ (kb/s)	1.67	4.2	Up to 2.5	Up to 100 (unrealistic considering 30 fps)	Up to 5
Rx Orientation	LOS link	LOS link	LOS link	LOS link	VLC: LOS link OCC: C_{off} with respect to distance
Average/ summarized performance	Low B efficiency	Effect of multilevel LED transmission based on varying amplitude depths need to be discussed	Signal attenuation due to use of bias-T needs to be solved.	Lacked details on simultaneous data transmission and processing	Improved B efficiency to twice that of 3-dB B_{LED}. Improved signal quality using V_d levels and lens characterization. Increased link span in experimental demonstration.

i.e., lower SNR and therefore increased BER. As a result, we have proposed an experimental hybrid OWC scheme that uses a bipolar multilevel OOK signal, as well as direct modulation with V_d levels and a lens characterization to improve the data throughput by increasing the system bandwidth to $2\times B_{\text{LED-3dB}}$, signal quality, and increasing the link span up to 4 m.

IV. CONCLUSION

In this paper, we demonstrated lab-scale experimental implementation and analyzed the performance of the hybrid OWC system for versatile IoT applications in an indoor static environment. A single red chip LED was used as a Tx for both VLC and OCC links. In the current work, we improved the throughput of the VLC link by up to ∼100 Mb/s, which corresponds to $2\times B_{\text{LED-3dB}}$ by means of direct modulation, different V_d levels, and optimizing the received optical power of the hybrid OWC link. While for the OCC link with different C_{off}, error-free data transmission was achieved for all values of $R_{b\text{-Low}}$ and L at A_{OL} values of 0 and 0.3. From the summary of results presented, based on the performance analysis, $0 < A_{\text{OL}} < 0.3$, $R_{b\text{-Low}}$ of 1 and 2 kb/s, $10 < R_{b\text{-High}} < 100$ Mb/s, and L of up to 4 m can be considered as the parameters with optimum values derived from the experimental demonstration of the proposed hybrid OWC scheme for versatile IoT environments. As a result of these values, the proposed scheme can be further implemented in real-life and extended IoT scenarios.

In addition, we addressed problems regarding the improvement of bandwidth efficiency (*i.e.,* R_b), the effect of multilevel LED transmission due to A_{OL}, and provided a comprehensive analysis for data processing for both VLC and OCC links. The proposed hybrid VLC-OCC SIMO scheme is envisioned to provide versatile optical-IoT based indoor services that allow users to receive data regardless of their device.

As part of potential future work, green and blue colors can be added to the red chip LED to generate white light while still transmitting through the red chip LED to maintain and improve the higher bandwidth. The chip LED can also be modulated considering an individual color channel and techniques such as polarization division multiplexing [13], equalization [16], and different modulation formats such as (*i*) orthogonal frequency division multiplexing [17] to improve R_b up to 1 Gb/s and 10 kb/s for VLC and OCC links, respectively; (*ii*) CDMA to support multi-user

environments [12]; and (iii) composite amplitude-shift keying that will allow different levels of shifts in A depths [18]. The scheme can also be tested for different types of PDs or camera-based orientations, along with long-link spans between the LED-based Tx and Rxs to support mobility in versatile optical-IoT environments.

REFERENCES

[1] G. Pan, J. Ye, and Z. Ding, "Secure hybrid VLC-RF systems with light energy harvesting," *IEEE Trans. Commun.*, vol. 65, no. 10, pp. 4348–4359, Oct. 2017.

[2] M. Z. Chowdhury, M. K. Hasan, M. Shahjalal, M. T. Hossan, and Y. M. Jang, "Optical wireless hybrid networks: Trends, opportunities, challenges, and research directions," *IEEE Commun. Surveys Tuts.*, vol. 22, no. 2, pp. 930–966, 2nd Quart., 2020.

[3] N. Chi, Y. Zhou, Y. Wei, and F. Hu, "Visible light communication in 6G: Advances, challenges, and prospects," *IEEE Veh. Technol. Mag.*, vol. 15, no. 4, pp. 93–102, Dec. 2020.

[4] P. Pesek, S. Zvánovec, P. Chvojka, Z. Ghassemlooy, and P. A. Haigh, "Demonstration of a hybrid FSO/VLC link for the last mile and last meter networks," *IEEE Photon. J.*, vol. 11, no. 1, pp. 1–7, Feb. 2019.

[5] Z. Huang, Z. Wang, M. Huang, W. Li, T. Lin, P. He, and Y. Ji, "Hybrid optical wireless network for future SAGO-integrated communication based on FSO/VLC heterogeneous interconnection," *IEEE Photon. J.*, vol. 9, no. 2, pp. 1–10, Apr. 2017.

[6] D. T. Nguyen, S. Park, Y. Chae, and Y. Park, "VLC/OCC hybrid optical wireless systems for versatile indoor applications," *IEEE Access*, vol. 7, pp. 22371–22376, 2019.

[7] M. K. Hasan, N. T. Le, M. Shahjalal, M. Z. Chowdhury, and Y. M. Jang, "Simultaneous data transmission using multilevel LED in hybrid OCC/LiFi system: Concept and demonstration," *IEEE Commun. Lett.*, vol. 23, no. 12, pp. 2296–2300, Dec. 2019.

[8] S. R. Teli, P. Chvojka, S. Vítek, S. Zvanovec, R. Perez-Jimenez, and Z. Ghassemlooy, "A SIMO hybrid visible-light communication system for optical IoT," *IEEE Internet Things J.*, vol. 9, no. 5, pp. 3548–3558, Mar. 2022.

[9] S. Teli, W. A. Cahyadi, and Y. H. Chung, "Optical camera communication: Motion over camera," *IEEE Commun. Mag.*, vol. 55, no. 8, pp. 156–162, Aug. 2017.

[10] M. K. Hasan, M. Shahjalal, M. Z. Chowdhury, M. T. Hossan, and Y. M. Jang, "Fuzzy logic based network selection in hybrid OCC/Li-Fi communication system," in *Proc. 10th Int. Conf. Ubiquitous Future Netw. (ICUFN)*, Prague, Czech Republic, Jul. 2018, pp. 95–99.

[11] M. K. Hasan, M. Z. Chowdhury, M. Shahjalal, and Y. M. Jang, "Fuzzy based network assignment and link-switching analysis in hybrid OCC/LiFi system," *Wireless Commun. Mobile Comput.*, vol. 2018, Nov. 2018, Art. no. 2870518.

[12] Y. Qiu, S. Chen, H. Chen, and W. Meng, "Visible light communications based on CDMA technology," *IEEE Wireless Commun.*, vol. 25, no. 2, pp. 178–185, Apr. 2018.

[13] P. Chvojka, A. Burton, P. Pesek, X. Li, Z. Ghassemlooy, S. Zvanovec, and P. A. Haigh, "Visible light communications: Increasing data rates with polarization division multiplexing," *Opt. Lett.*, vol. 45, no. 11, pp. 2977–2980, Jun. 2020.

[14] W. Ozan, R. Grammenos, and I. Darwazeh, "Zero padding or cyclic prefix: Evaluation for non-orthogonal signals," *IEEE Commun. Lett.*, vol. 24, no. 3, pp. 690–694, Mar. 2020.

[15] Y. Liu, "Decoding mobile-phone image sensor rolling shutter effect for visible light communications," *Opt. Eng.*, vol. 55, no. 1, Jan. 2016, Art. no. 016103.

[16] X. Li, Z. Ghassemlooy, S. Zvanovec, R. Perez-Jimenez, and P. A. Haigh, "Should analogue pre-equalisers be avoided in VLC systems?" *IEEE Photon. J.*, vol. 12, no. 2, pp. 1–14, Apr. 2020.

[17] T. Nguyen, M. D. Thieu, and Y. M. Jang, "2D-OFDM for optical camera communication: Principle and implementation," *IEEE Access*, vol. 7, pp. 29405–29424, 2019.

[18] Y. Yang and J. Luo, "Composite amplitude-shift keying for effective LED-camera VLC," *IEEE Trans. Mobile Comput.*, vol. 19, no. 3, pp. 528–539, Mar. 2020.

SHIVANI RAJENDRA TELI received the bachelor's degree from Savitribai Phule Pune University, Maharashtra, India, in 2015, the M.Sc. degree from the Department of Information and Communications Engineering, Pukyong National University, Busan, South Korea, in 2018, and the Ph.D. degree from the Faculty of Electrical Engineering, Czech Technical University (CTU) in Prague, in 2021, within "Visible light-based interoperability and networking (ViSIoN)," which is a project under the European Union's Horizon H2020 Marie Skłodowska-Curie Innovative Training Network (MSCA ITN). She is currently a Postdoctoral Researcher with the CTU Global Fellowship Program. Her research interests include wireless communication systems, visible light communications, and optical camera communications for the Internet of Things and sensor networks.

CARLOS GUERRA-YANEZ received the M.Eng. degree from Universidad de Las Palmas de Gran Canaria, Spain, in 2021. He is currently pursuing the Ph.D. degree with the Wireless and Fiber Optics Group, Czech Technical University in Prague, Czech Republic. His current research interests include signal processing, modulation techniques, and channel coding for visible light communications as well as quantum key distribution over free space optics.

VICENTE MATUS ICAZA received the degree in electrical engineering from the University of Chile, in 2018, and the Ph.D. degree from the University of Las Palmas de Gran Canaria (ULPGC), Spain, in 2021. He was a Marie S. Curie Fellow with the Horizon 2020 Program of the European Union for the ITN-VISION Project. He is currently a Researcher with the Photonics Division, Institute for Technological Development and Innovation in Communications (IDeTIC), ULPGC, and a Visiting Researcher with Instituto de Telecomunicações Aveiro, Portugal, funded by the Catalina Ruiz 2022 Scholarship from the Canary Islands Government. His research interests include the experimental development and deployment of optical wireless communication systems, specifically those based on using cameras as receivers (optical camera communication) and their outdoor applications for wireless sensor networks. Among the applications of his interest are the automation of agriculture systems, vehicular communication, and wearable sensors for medical applications.

RAFAEL PEREZ-JIMENEZ was born in Madrid, in 1965. He received the M.S. degree from Universidad Politécnica de Madrid, Spain, in 1991, and the Ph.D. degree (Hons.) from Universidad de Las Palmas de Gran Canaria (ULPGC), Spain, in 1995. He is currently pursuing the Ph.D. degree in telecommunications history with Universidad de La Laguna. He is a Full Professor with ULPGC, where he leads the IDeTIC Research Institute. His current research interests include optical camera communications (OCC), optical indoor channel characterization, and the design of robust visible light communications (VLC) systems for indoor communications, especially applied for sensor interconnection and positioning. He received the Gran Canaria Science Prize, in 2007, the Vodaphone Foundation Research Award, in 2010, and the RSEAPGC Honor Medal, in 2017.

ZABIH GHASSEMLOOY (Senior Member, IEEE) received the B.Sc. degree (Hons.) in electrical engineering from Manchester Metropolitan University, in 1981, and the M.Sc. and Ph.D. degrees from The University of Manchester, U.K., in 1984 and 1987, respectively. From 1987 to 1988, he was a Postdoctoral Research Fellow with the City, University of London, U.K. From 1988 to 2004, he was with Sheffield Hallam University, U.K. From 2004 to 2014, he was an Associate Dean (Research) with the Faculty of Engineering and Environment, Northumbria University, U.K., where he is currently the Head of Optical Communications Research Group. Since 2016, he has been a Research Fellow with the Chinese Academy of Sciences, where he has been a Distinguished Professor, since 2015. He has published over 980 papers (more than 425 journals and eight books) with several best paper awards, given more than 100 keynote/invited talks, and supervised 12 research fellows and 75 Ph.D. students. His research interests include optical wireless communications, free space optics, visible light communications, and hybrid RF and optical wireless communications. He is a fellow of SOA and IET. He was the Vice-Chair of EU Cost Action IC1101 (2011–2016). He is the Vice-Chair of the EU COST Action CA19111 NEWFOCUS (European Network on Future Generation Optical Wireless Communication Technologies; 2020–2024). He is the Chief Editor of the *British Journal of Applied Science and Technology* and the *International Journal of Optics and Applications*, an associate editor of a number of international journals, and the co-guest editor of a number of OWC special issues. He has been the Vice-Chair of the OSA Technical Group of Optics in Digital Systems, since 2018. He has been the Chair of the IEEE Student Branch, Northumbria University, Newcastle upon Tyne, since 2019. From 2004 to 2006, he was the IEEE U.K./IR Communications Chapter Secretary, the Vice-Chairman (2006–2008), the Chairman (2008–2011), and the Chairman of the IET Northumbria Network (2011–2015).

STANISLAV ZVANOVEC (Senior Member, IEEE) received the M.Sc. and Ph.D. degrees from the Faculty of Electrical Engineering, Czech Technical University (CTU) in Prague, in 2002 and 2006, respectively. He is currently a Full Professor and the Deputy Head of the Department of Electromagnetic Field and the Chairperson of the Ph.D. Branch, CTU. He is the author of two books (and the coauthor of the recent book *Visible Light Communications: Theory and Applications*), several book chapters, and more than 300 journals and conference papers. His current research interests include free space optical and fiber optical systems, visible light communications, OLED, RF over optics, and electromagnetic wave propagation issues for millimeter wave bands.